Effects of wetting and anchoring on capillary phenomena in a confined liquid crystal

D. de las Heras
Departamento de Física Teórica de la Materia Condensada, Universidad Autónoma de Madrid, E-28049 Madrid, Spain

E. Velasco
Departamento de Física Teórica de la Materia Condensada and Instituto de Ciencia de Materiales Nicolás Cabrera, Universidad Autónoma de Madrid, E-28049 Madrid, Spain

L. Mederos
Instituto de Ciencia de Materiales, Consejo Superior de Investigaciones Científicas, E-28049 Cantoblanco, Madrid, Spain

(Received 13 November 2003; accepted 12 December 2003)

A fluid of hard spherocylinders of length-to-breadth ratio $L/D=5$ confined between two identical planar, parallel walls—forming a pore of slit geometry—has been studied using a version of the Onsager density-functional theory. The walls impose an exclusion boundary condition over the particle's centers of mass, while at the same time favoring a particular anchoring at the walls, either parallel or perpendicular to the substrate. We observe the occurrence of a capillary transition, i.e., a phase transition associated with the formation of a nematic film inside the pore at a chemical potential different from μ_b—the chemical potential at the bulk isotropic–nematic transition. This transition terminates at an Ising-type surface critical point. In line with previous studies based on the macroscopic Kelvin equation and the mesoscopic Landau–de Gennes approach, our microscopic model indicates that the capillary transition is greatly affected by the wetting and anchoring properties of the semi-infinite system, i.e., when the fluid is in contact with a single wall or, equivalently, the walls are at a very large distance. Specifically, in a situation where the walls are preferentially wetted by the nematic phase in the semi-infinite system, one has the standard scenario with the capillary transition taking place at chemical potentials less than μ_b (capillary nematization transition or capillary ordering transition). By contrast, if the walls tend to orientationally disorder the fluid, the capillary transition may occur at chemical potentials *larger* than μ_b, in what may be called a *capillary isotropization* transition or capillary disordering transition. Moreover, the anchoring transition that occurs in the semi-infinite system may affect very decisively the confinement properties of the liquid crystal and the capillary transitions may become considerably more complicated. [DOI: 10.1063/1.1646374]

I. INTRODUCTION

The confinement properties of fluids are very important to understand many natural phenomena and industrial processes. Particularly interesting, both from practical and fundamental reasons, are the properties of liquid-crystal forming materials that are confined by two walls.[1] These may induce some preferred orientations in the nematic director which may compete with the interactions in the liquid crystal to give the final structure in the pore.[2] Therefore, the confinement brings about a new element which modifies the wetting and orientation properties of the fluid.

In pioneering work, Sheng,[3] and later Poniewierski and Sluckin,[2] predicted a phenomenon similar to the capillary condensation of liquid from vapor in confined simple fluids, but involving the isotropic and nematic phases of liquid crystals. Poniewierski and Sluckin[4] extended the analysis of Sheng and shown, using a mesoscopic Landau–de Gennes formalism, that the nematic–isotropic transition temperature of a liquid crystal placed between two parallel walls may increase or decrease, with respect to the bulk value, as the distance between the walls decreases, depending on the wetting conditions prevailing at the walls. This effect, well accounted for by the analogue of the Kelvin equation, is similar to the capillary condensation/evaporation transitions occurring in simple argonlike fluids and more complex fluids such as water.[5] Recently the capillary condensation of a thermotropic nematic liquid crystal and the associated first-order transition line terminating in a critical point was observed by Kocevar *et al.* using atomic force microscopy.[6]

The interest of capillary studies of complex fluids, and liquid crystals in particular, lies in their intrinsic importance to understand wetting and flow properties of nanometer-scale films and their implications in liquid-crystal colloidal dispersions and emulsions. For example, colloidal dispersions in a liquid-crystalline hosts exhibit interesting rheological and optical properties from the point of view of applications; these properties are caused by the peculiar interparticle forces mediated by the liquid-crystalline host, arising either from nematic director deformations or by nematic capillary condensation in the isotropic phase. These effects may be

relevant for potential applications such as self-assembly of complex materials and systems with remarkable optical properties.

In this paper we have examined the confinement properties of a liquid-crystalline material using a microscopic interaction model based on the simple hard-spherocylinder model together with a version of the Onsager density-functional theory. We consider a fluid of hard spherocylinders of length-to-breadth ratio $L/D=5$ confined by two identical, planar, parallel walls—in the so-called slit geometry—that act as hard walls on the centres of mass of the particles and additionally can orient the particles along some predetermined direction. This model has been analyzed previously[7] and shown to exhibit a rich surface phase diagram with wetting and reentrant wetting transitions, anchoring, and prewetting transitions. These phenomena are obtained as the chemical potential and surface affinity of the walls are varied. Here we examine how these properties affect and are affected by the confinement of the system.

Recently a few theoretical studies have focused on the confinement properties of fluids made up of simple model particles, using either density-functional theory or computer simulation.[8–13] For example, Chrzanowska *et al.*[14] have recently analyzed the structure of a fluid of hard Gaussian overlap molecules between parallel hard walls, both using the Onsager density-functional theory and computer simulation. Also, van Roij *et al.*[15–17] have used computer simulation and a Zwanzig approximation on the Onsager theory to investigate the capillary nematization transition of a hard spherocylinder fluid confined between parallel hard walls. All of these studies have not explored different scenarios, in particular, the interplay between the wetting behavior of the fluid and confinement. In this respect, we believe our work to be the first to address these questions from a completely molecular point of view, without restricting the calculations to any simplifying assumption about the orientations of the particles.

The remainder of the paper is organized as follows: In the following section, we present the theoretical model and provide a few technical details; a more detailed account of the model has been presented elsewhere.[7] In Sec. III we present the results, and finally in Sec. IV we give the conclusions and present a few lines for future research.

II. SOME THEORETICAL DETAILS

In this section we briefly sketch the theory and present some numerical details. For a more detailed account of the theory see Refs. 7, 18–20. The relevant free energy density functional for our confinement problem is the grand canonical free energy, $\Omega[\rho]=F[\rho]-\mu N$, where F is the Helmholtz free energy, μ the imposed chemical potential, N the number of molecules and $\rho(\mathbf{r},\hat{\mathbf{\Omega}})$. In the present work we use an extension of Onsager theory[21] to obtain the Helmholtz free energy, which is the central quantity to approximate. The extended theory allows for slowly-varying molecular distributions of the type that are expected in the confined liquid crystal close to the isotropic–nematic transition. The Helmholtz free-energy density functional is approximated by

$$F[\rho]=F_{\mathrm{id}}[\rho]+kT\int\int d\mathbf{r}d\hat{\mathbf{\Omega}}\rho(z,\hat{\mathbf{\Omega}})\times\left[\frac{\Delta\Psi(\rho(z))}{\frac{4\pi}{3}\rho(z)\sigma_{\mathrm{eq}}^3}\right]\int\int d\mathbf{r}'d\hat{\mathbf{\Omega}}'v_{\mathrm{exc}}(\mathbf{r}-\mathbf{r}',\hat{\mathbf{\Omega}},\hat{\mathbf{\Omega}}')\times\rho(z',\hat{\mathbf{\Omega}}')+\int d\mathbf{r}d\hat{\mathbf{\Omega}}\rho(z,\hat{\mathbf{\Omega}})v_{\mathrm{ext}}(z,\hat{\mathbf{\Omega}}),\tag{1}$$

where v_{exc} is the overlap function for two HSPC (unity if they overlap and zero otherwise), $\Delta\Psi(\rho(z))$ is a prefactor that depends on the angular-averaged density distribution $\rho(z)$,

$$\rho(z)\equiv\int d\hat{\mathbf{\Omega}}\rho(z,\hat{\mathbf{\Omega}})\tag{2}$$

and v_{ext} is the external potential representing the effect of the two substrates on a single molecule,

$$v_{\mathrm{ext}}(z,\hat{\mathbf{\Omega}})=\begin{cases}\infty, & z<0,\ z>H\\ V_0[e^{-\alpha z}+e^{-\alpha(H-z)}]P_2(\hat{\mathbf{\Omega}}\cdot\hat{\mathbf{z}}), & 0\leqslant z\leqslant H,\end{cases}\tag{3}$$

where H is the pore width, i.e., the distance between the two parallel walls, V_0 the substrate strength parameter, α the decay inverse length, $\hat{\mathbf{z}}$ the unit vector normal to the walls, and $P_2(x)$ the second-order Legendre polynomial. The parameter σ_{eq} is an effective particle diameter (see Refs. 18–20 for a discussion). Here we have chosen z to be along the normal to the substrates and with origin in the substrate at the left, so that our density distributions only depend on that coordinate since the substrate is chosen not to possess any transverse structure. $F_{\mathrm{id}}[\rho]$ is the ideal-gas free-energy density functional which is exactly given by

$$F_{\mathrm{id}}[\rho]=kT\int d\mathbf{r}d\hat{\mathbf{\Omega}}\rho(z,\hat{\mathbf{\Omega}})[\log\rho(z,\hat{\mathbf{\Omega}})-1]\tag{4}$$

with T the temperature and k the Boltzmann's constant. As usual we introduce an angular distribution function $f(z,\hat{\mathbf{\Omega}})$ by $\rho(z,\hat{\mathbf{\Omega}})=\rho(z)f(z,\hat{\mathbf{\Omega}})$ and work not with the function itself but with the first moments relevant for axisymmetric molecules,

$$\eta_m(z)=\int d\hat{\mathbf{\Omega}}f(z,\hat{\mathbf{\Omega}})Y_{2m}(\hat{\mathbf{\Omega}}),\quad m=0,\pm1,\pm2\tag{5}$$

with Y_{lm} a spherical harmonic. Assuming mirror symmetry with respect to the xz plane, the only significant moments are three; transforming to a reference frame where the new z axis lies along the local director the three relevant moments are $\psi(z)$, the angle between the director $\hat{\mathbf{n}}$ and the unit vector normal to the substrate, $\hat{\mathbf{z}}$, and two distributions that represent the ordering around the local director: $\eta(z)$ (uniaxial order parameter) and $\sigma(z)$ (biaxial order parameter). These order-parameter functions, together with the local density $\rho(z)$, define the configurational state of our adsorption system. Details on how the free energy is calculated in terms of these order parameters can be obtained from Refs. 18–20.

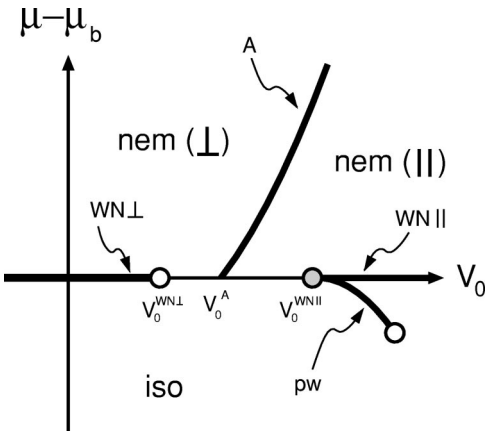

FIG. 1. Pictorial representation of the surface phase diagram of the model of hard spherocylinders in the presence of a single wall. The phase diagram includes the wetting and anchoring properties of the semi-infinite model in the chemical potential (μ)–surface strength parameter (V_0) plane. The chemical potential is referred to the value at isotropic-nematic coexistence, μ_b. The horizontal axis thus represents bulk coexistence. On this axis wetting transitions by nematic with director perpendicular to the wall (WN$\perp$) and by nematic with director parallel to the wall (WN$\parallel$) are represented by thick lines. Off-coexistence phase transitions include the anchoring transition (A) and the prewetting transition (pw) associated to the bulk WN$\parallel$ wetting transition (which is of first order). Equilibrium phases in bulk are labeled as ''iso'' (isotropic), ''nem ($\perp$)'' (nematic with director perpendicular to the wall) and ''nem ($\parallel$)'' (nematic with director parallel to the wall).

Once the external potential representing the effect of the substrates is specified, the resulting grand-potential free-energy functional $\Omega([\rho];\mu)$ can be minimized numerically with respect to the four order-parameter distributions, for fixed bulk conditions, i.e., for fixed chemical potential μ (T is not a relevant thermodynamic variable since our molecular model is hard).

The length scale used in this paper have been taken to be σ_{eq}, the effective particle diameter.[18–20] For the particle chosen in this study, with $L/D=5$, the numerical value is $\sigma_{\mathrm{eq}}=2.04D=0.41L$. A final comment on the model is that it possesses a certain degree of nonlocality through the overlap function V_{exc}, but this is not sufficient to reproduce the density variations that are expected in a high-density fluid near a wall. A more sophisticated theory, of the weighted-density type, would be necessary to account for these structural effects. The failure of our theory in this respect is reflected in the violation of the sum rule relating the pressure with the density value at contact in the semi-infinite system (see Ref. 7). This feature, however, is not expected to be serious at the qualitative level since we want to focus on the orientational properties of the fluid.

III. RESULTS

Figure 1 gives a pictorial representation of the surface phase diagram of the model in the chemical potential (μ)—surface strength parameter (V_0) plane when the fluid is in contact with a single wall; this problem has been analyzed in Ref. 7. The chemical potential is referred to the value at isotropic–nematic coexistence, μ_b. Thus, we have coexistence conditions on the horizontal axis. Bulk wetting transitions are indicated by thick solid lines. Depending on the value of V_0 the substrate can be wet by a nematic film with homeotropic orientation (WN$\perp$), or with parallel orientation (WN$\parallel$). The associated wetting transitions are located at $V_0=V_0^{\mathrm{WN}\perp}\equiv 0$ and $V_0=V_0^{\mathrm{WN}\parallel}\equiv 0.48kT$, and are of second and first order, respectively. Off-coexistence surface phase transitions include the anchoring transition (A) in the bulk nematic region, separating phases with different director alignments, and the prewetting transition associated with the WN$\parallel$ wetting transition, which is of first order (by contrast, since the WN$\perp$ wetting transition appears to be of second order, it has no associated prewetting line). The surface behavior of the model, embodied in the wetting and anchoring transitions shown in Fig. 1, is crucial to understand the phenomena that arise when the fluid is confined.

Next we confine the fluid between two planar, identical, parallel walls, separated by a distance H, and search for solutions of the density functional as a function of chemical potential μ, the surface strength parameter V_0, and the distance between the walls H. What we are looking for is the global phase behavior of the fluid when confined between the walls. In order to analyze the confinement properties of the model we have chosen to obtain the phase diagram in the $\mu-H$ plane for different values of V_0, having as a guide the surface phase diagram for $H=\infty$, i.e., Fig. 1.

In Fig. 2 we plot some profiles pertaining to the case $V_0=-0.1kT$, $H=35.4\sigma_{\mathrm{eq}}$. This value of the surface strength parameter corresponds to wetting by nematic with homeotropic orientation in the semi-infinite system (see Fig. 1). Figure 2(a) shows the nematic order-parameter profiles, whereas Fig. 2(b) shows the number density profiles. Each of the graphs contains four profiles. Those represented by dashed lines correspond to fluid states that, with the same chemical potential, $\mu\equiv\mu(H)=0.987\mu_b$ (μ_b is the chemical potential at which the bulk isotropic–nematic transition takes place), have the same grand potential: they coexist at a first-order phase transition. In Fig. 2(a) we can see that one of the profiles has a zero value of the nematic order parameter in the central region of the pore, corresponding to an isotropic fluid; the other has a high value of the order parameter in the whole pore, which can be associated with a nematic fluid. The structure of the fluid in the regions next to the two walls is quite similar in all cases and does not change significantly. The profiles represented by continuous lines correspond to states with a lower chemical potential, $\mu<\mu(H)$, and a higher chemical potential, $\mu>\mu(H)$, than that at which the capillary transition occurs. This behavior clearly demonstrates the existence of a first-order capillary nematization transition at a chemical potential $\mu(H)$, at which the structure of the confined film changes discontinuously: the nematic order parameter in the central region changes from zero to a value compatible with the corresponding value in bulk. The associated change in density, Fig. 2(b), is by contrast very small. We will refer to the phases in the confined system as ''nematic'' and ''isotropic'' depending on whether the nematic adsorption is large or small, despite the fact that in the latter case there may be a adsorbed layer with high nematic order parameter close to the walls, see Fig. 2(a). The nematic adsorption Γ is defined in terms of the spatial integral of the nematic order-parameter profile,

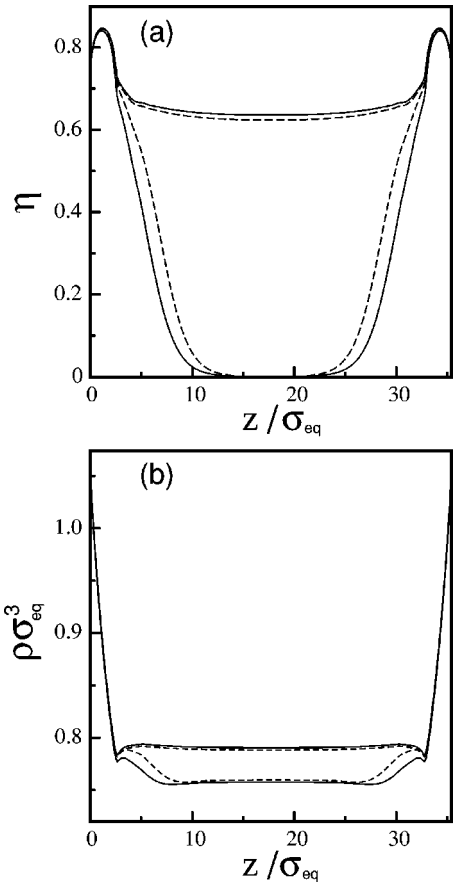

FIG. 2. Nematic order parameter (a) and density (b) profiles for the case where homeotropic orientation obtains at the substrates ($V_0=-0.1kT$) and for a pore width $H=35.4\sigma_{\mathrm{eq}}$. In this regime there is wetting by nematic with homeotropic orientation in the semi-infinite system. Four profiles are represented in each case. Those represented by continuous lines correspond to states below and above the capillary nematization transition, at chemical potentials $\mu=0.98\mu_b$ and $\mu=0.99\mu_b$. The profiles represented by discontinuous lines correspond to coexisting states at $\mu=0.987\mu_b$. The value of the substrate decay inverse length was taken as $\alpha=0.3\sigma_{\mathrm{eq}}^{-1}$.

$$\Gamma=\frac{1}{H}\int_0^H dz\,\eta(z). \tag{6}$$

In Fig. 3 the nematic adsorption is represented as a function of chemical potential for the case $V_0/kT=-0.1$ and $H=35.4\sigma_{\mathrm{eq}}$. The vertical line indicates the position of the capillary phase transition and both the thermodynamically stable branches and their metastable extensions are shown.

The surface phase diagram in the chemical potential (μ)–pore width (H) plane is shown in Fig. 4. Capillary transition lines have been plotted for different values of the surface strength parameter V_0 in the range $-0.1\leqslant V_0/kT\leqslant 0.2$. As expected from macroscopic arguments (see below), all transition lines tend to be horizontal in the limit $H\to\infty$ and asymptotically tend to the chemical potential at coexistence, μ_b. This indicates that, in this limit, the usual bulk isotropic–nematic transition is recovered. The shift of the transition chemical potential from the bulk value, $\Delta\mu(V_0,H)\equiv\mu(V_0,H)-\mu_b$, depends on the value of the pore width H and the nature of the walls, here given by the strength (V_0) and decay (α) parameters—throughout this work we take the decay parameter α to be fixed at a value

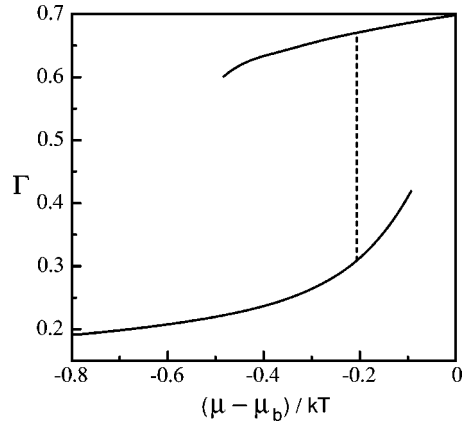

FIG. 3. Nematic adsorption as a function of chemical potential for a confined fluid with pore width $H=35.4\sigma_{\mathrm{eq}}$ and a surface strength parameter $V_0/kT=-0.1$. The vertical line gives the location of the thermodynamic capillary transition. The value of the substrate decay inverse length was taken as in Fig. 2.

$0.3\sigma_{\mathrm{eq}}^{-1}$. The analog of the Kelvin equation for the liquid–vapor transition in a confined geometry can be obtained for the nematic–isotropic transition using a macroscopic analysis of the problem ($H\to\infty$). This approach was first worked out by Poniewierski and Sluckin[4] for thermotropic liquid crystals. For our (athermal) hard-spherocylinder fluid a parallel derivation results in the following behavior for $\Delta\mu(V_0,H)$:

$$\Delta\mu(V_0,H)\to\frac{2(\gamma_{SN}^{\perp}-\gamma_{SI})}{(\rho_N-\rho_I)H}, \tag{7}$$

where $\gamma_{SN}^{\perp}$, γ_{SI} are the surface tensions of the wall-nematic and wall-isotropic interfaces, respectively, in the semi-infinite system, and ρ_N, ρ_I are the densities of the nematic

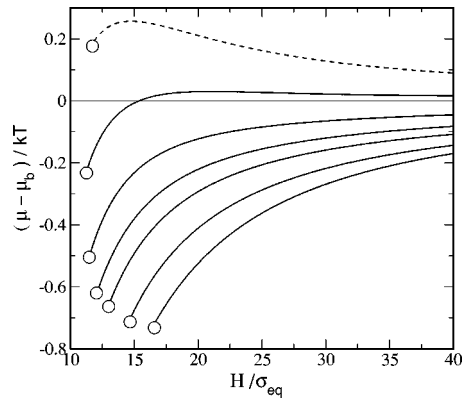

FIG. 4. Surface phase diagram in the chemical potential (μ)–pore width (H) plane for the case of homeotropic director alignment. The chemical potential is referred to the coexistence value μ_b and expressed in thermal energy units. Lines indicate the location of the capillary transition from isotropic (below the corresponding line) to nematic (above the corresponding line) for different values of the surface strength parameter V_0. From bottom to top: $V_0/kT=-0.10$, -0.05, 0.00, 0.03, 0.07, 0.13, and 0.20. The case $V_0/kT=0.20$ is plotted using a dashed line, which indicates that the corresponding transition line is metastable with respect to parallel director alignment. Open circles indicate the approximate location of the critical point for each case. The value of the substrate decay inverse length was taken as $\alpha=0.3\sigma_{\mathrm{eq}}^{-1}$.

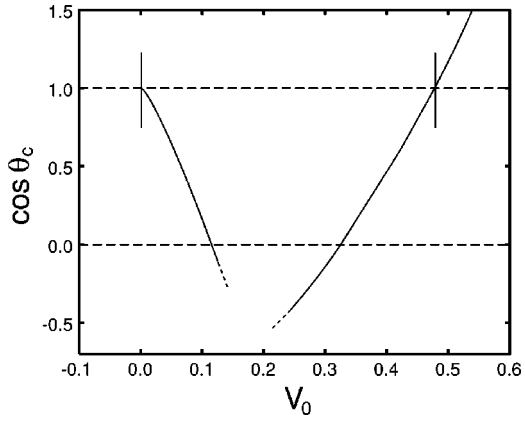

FIG. 5. Behavior of the cosine of the contact angle θ_c as a function of the substrate strength parameter V_0 in the semi-infinite system. Dashed lines indicate that the continuous lines are supposed to be extended further, but that they have not been calculated explicitely. Short vertical lines indicate the location of the two wetting transitions. Value of the substrate decay inverse length as in Fig. 2.

and isotropic phases, all at coexistence conditions. The superscript $\perp$ in $\gamma_{SN}^{\perp}$ indicates that the equilibrium nematic director configuration has been arbitrarily chosen to be homeotropic; in any case the surface tension γ_{SN} should conform to the equilibrium director orientation. A discussion along the same lines as in Ref. 2 can now be made. First, since $\rho_N > \rho_I$, the sign of $\Delta\mu$ is dictated by the sign of $\gamma_{SN}^{\perp} - \gamma_{SI}$. Consider a situation of partial wetting by a nematic phase with homeotropic orientation. Then, $\gamma_{SI} = \gamma_{SN}^{\perp} + \gamma_{NI}\cos\theta_c$, where γ_{NI} is the surface tension of the nematic–isotropic interface and θ_c is the contact angle. We have $\gamma_{SN}^{\perp} - \gamma_{SI} = -\gamma_{NI}\cos\theta_c$ and the Kelvin equation can be written

$$\Delta\mu(V_0,H) \to -\frac{2\gamma_{IN}\cos\theta_c}{(\rho_N-\rho_I)H}. \tag{8}$$

Since our our density-functional results should verify the limits established by the Kelvin equation, we may use the values of the contact angle derived from our density-functional theory to predict the sign of $\Delta\mu$. The behavior of $\cos\theta_c$ as a function of V_0 is plotted in Fig. 5. The location of the two wetting transitions is indicated by short vertical lines at $V_0^{\mathrm{WN}\perp}$ (wetting by nematic with homeotropic director alignment) and $V_0^{\mathrm{WN}\parallel}$ (wetting by nematic with parallel director alignment). At these transitions $\cos\theta_c = 1$. In the partial-wetting regime $\cos\theta_c$ changes sign at two values of V_0, which are approximately $V_0^c/kT = 0.12$ and $V_0^{c\prime}/kT = 0.32$. Therefore, we have the following régimes at large H:

(1) $V_0^{\mathrm{WN}\perp} \leqslant V_0 < V_0^c$ or $V_0^{c\prime} < V_0 \leqslant V_0^{\mathrm{WN}\parallel}$: $\cos\theta_c > 0$, which implies $\gamma_{SN}^{\perp} < \gamma_{SI}$ or $\gamma_{SN}^{\parallel} < \gamma_{SI}$, and the capillary transition proceeds in the usual manner, with $\Delta\mu < 0$, i.e., the nematic–isotropic transition occuring at chemical potentials lower than the bulk value, $\mu(H) < \mu_b$: this is a *capillary nematization* transition.

(2) $V_0^c < V_0 < V_0^{c\prime}$: $\cos\theta_c < 0$, which implies $\gamma_{SN}^{\perp} > \gamma_{SI}$ or $\gamma_{SN}^{\parallel} > \gamma_{SI}$, and the capillary transition proceeds in a reversed manner, with $\Delta\mu > 0$, i.e., the nematic–isotropic transition occuring at chemical potentials higher than the bulk value, $\mu(H) > \mu_b$: this is a *capillary isotropization* transition.

This behavior is therefore governed by the relative values of the two surface tensions γ_{SI} and $\gamma_{SN}^{\perp}$; when adsorption of the nematic phase is more favourable than adsorption of the isotropic phase ($\gamma_{SI} > \gamma_{SN}^{\perp}$) the surface free energy compensates the free-energy cost associated with having a nematic film at too low a chemical potential. Close to the wetting transition by nematic, but in the partial wetting régime, the preference of the substrate changes from nematic to isotropic adsorption ($\gamma_{SI} < \gamma_{SN}^{\perp}$) and a capillary isotropisation transition takes place. This behavior is already apparent in Fig. 4 for H larger than $40\sigma_{\mathrm{eq}}$ (note that the case $V_0/kT = 0.13$ is already above the critical value of V_0^c where the change in $\cos\theta_c$ takes place). The discussion applies when H is large; as H is reduced the macroscopic Kelvin equation breaks down and has to be corrected by terms that account for the interaction between the two interfaces. Our density-functional results indicate that there may be a *reentrant* capillary nematization transition when the pore is sufficiently narrow. For example, in the case $V_0/kT = 0.13$ there is a maximum in the transition line which for very narrow pores decreases, implying that the interaction between the two interfaces is constructive and promotes nematic formation in the pore. More generally, for narrow pores one would expect effective interface interactions and changes with respect to the macroscopic behavior. One has to bear in mind, however, that our density-functional model cannot account for the strong inhomogeneities that occur next to the walls in this isotropic–nematic system (high number density) and that, consequently, effects related to interaction between the walls mediated by the intervening liquid when the pore width is small will not be properly treated.

The complex capillary behavior of the present system, with capillary nematization and isotropization transitions, and reentrant capillary transitions as the surface strength parameter of the walls is varied, is the result of the peculiar wetting properties of the system. In simple fluids adsorbed on a substrate there may be only one wetting transition by the liquid phase and maybe a drying transition (wetting by the vapor phase). The cosine of the contact angle only changes sign once, giving rise to capillary condensation and capillary evaporation transitions in the confined system. In our liquid-crystalline system two wetting transitions by nematic phases with different alignment characteristics are present in the system and, unavoidably, $\cos\theta_c$ changes sign twice. Note, in addition, that the nematic–isotropic surface tension γ_{NI} is very small in these systems and, consequently, $\cos\theta_c$ varies very rapidly with the surface parameters, in contrast with the situation in simple fluids where the liquid-vapor surface tension is generally high far from the critical point.

An interesting feature of the capillary transitions involves the existence of critical points (μ_c, H_c) terminating the capillary isotropic–nematic transition, and how these critical points behave as the surface strength parameter V_0 is varied. This feature was predicted by Sheng[3] in his pioneer-

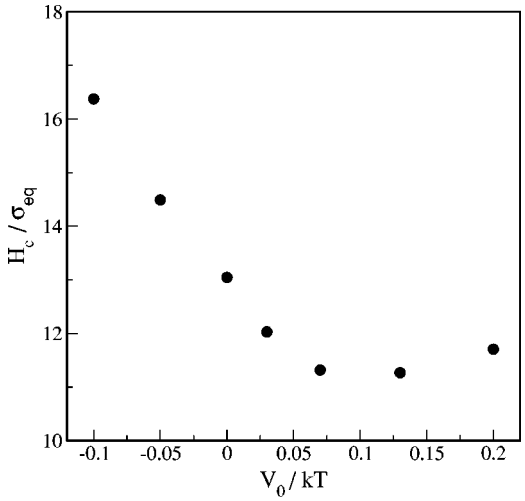

FIG. 6. Behavior of the critical pore width H_c as a function of the substrate strength parameter V_0 for the case of homeotropic director alignment. Substrate decay inverse length was taken to be $\alpha = 0.3\sigma_{eq}^{-1}$.

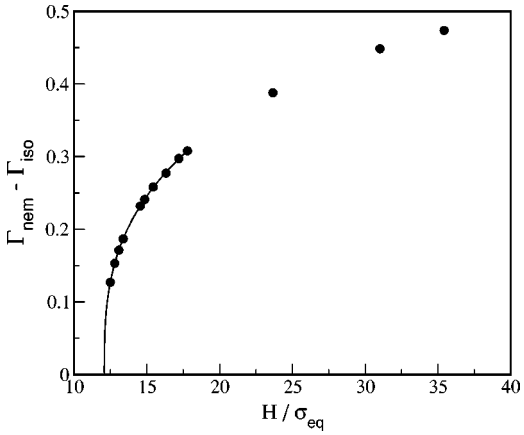

FIG. 7. Difference in nematic adsorption $\Gamma_{nem} - \Gamma_{iso}$ between the nematic and isotropic phases inside the pore as a function of pore width H for the case of homeotropic director alignment and for a value of the substrate strength parameter $V_0/kT = 0.03$. The line is a best fit, restricted to the first seven points, to a form $\Gamma_{nem} - \Gamma_{iso} = a(H/\sigma_{eq} - b)^{\beta}$ with $a = 0.1711$, $b = 12.079$, and $\beta = 0.3372$.

ing work and is probably generic. Figure 6 represents the evolution of H_c with V_0. The plot shows two régimes: for $V_0/kT < 0.03$ the critical width H_c decreases more or less linearly, whereas for $V_0/kT > 0.03$ the variation of the critical width tends to flatten off. It is tempting to speculate that the two regimes are related to the existence of the wetting transition in the semi-infinite system. When complete wetting at coexistence occurs ($V_0 < 0$) relatively thick nematic layers develop at the walls, even in the confined system at off-coexistence conditions. We may argue, loosely speaking, that the capillary transition will occur when the two nematic films more or less meet at the center of the pore, which will occur for more narrow pores as V_0 increases from negative values (remember that the associated wetting transition is of second order at bulk coexistence, and consequently nematic films adsorbed at the walls in the confined system and off coexistence are expected to become thinner as V_0 increases toward zero from negative values). Once we are out of the wetting regime at coexistence ($V_0 > 0$) the thickness of the nematic layers is approximately constant or at least grows relatively slowly, the surface films consisting of a single layer of homeotropically oriented particles. The two layers then meet when the pore width is approximately equal to two layer thicknesses.

The nature of the critical points can be ascertained by looking at the behavior of the nematic order parameter as the critical point is approached. The difference in nematic adsorption $\Gamma_{nem} - \Gamma_{iso}$ between the nematic and isotropic phases inside the pore as a function of the pore width H along the transition line is plotted in Fig. 7 for the case $V_0/kT = 0.03$ (the middle case in Fig. 4). This quantity approaches zero at the critical point as $\Gamma_{nem} - \Gamma_{iso} \sim (H - H_c)^{\beta}$, where β is an exponent. A least-square fit of our data to this form (see Fig. 7) gives $\beta = 0.3372$. This is compatible with the mean-field exponent for the two-dimensional Ising model ($\beta = 1/3$), which is in the same universality class as the capillary transition.

Simulations by Dijkstra *et al.*[15] for a fluid of hard spherocylinders with $L/D = 15$ confined by two parallel hard walls indicate the presence of a capillary nematization transition. Their study is based on a Gibbs-ensemble technique for confined systems, and they do not measure the chemical potential. Interestingly, they observe the presence of a critical point such that, for wall separations less than a critical value, no nematization transition occurs. The critical pore width estimated by Dijkstra *et al.* is such that $H_c/(L+D) = 2.3$, i.e., about two molecular lengths, whereas in our case $H_c/\sigma_{eq} \approx 13$ for $V_0 = 0$ (see Fig. 5); since $\sigma_{eq} = 2.04D$, this gives $H_c/(L+D) \approx 4.4$. This comparison is not entirely significant, since our calculations are performed on spherocylinders of very different aspect ratio, $L/D = 5$, and the walls are modelled in a very different way (true hard walls in the case of Ref. 15 and hard walls only on the centers of mass in the present work).

The results contained in Fig. 4 were obtained using initial profiles consistent with a homoeotropic director configuration. These initial profiles always gave rise to equilibrium solutions with the same homeotropic configuration that are, therefore, associated with local mimima of the functional. However, according to Fig. 1, there is an anchoring transition in the semi-infinite system at a value $V_0 = V_0^A \approx 0.17kT$ in bulk nematic conditions and at coexistence. The transition is of first order and involves a discontinuous change of the nematic director orientation from perpendicular (homeotropic) to parallel with respect to the wall. The last value of V_0 for which the capillary nematization transition is shown in Fig. 4 ($V_0/kT = 0.20$) is clearly above the anchoring transition in the semi-infinite system at coexistence, whereas the previous one ($V_0/kT = 0.13$) is below this anchoring transition (in fact, we have checked that the anchoring transition shows only a weak dependence on the pore width and the value of the chemical potential, except possibly for very narrow pores). This may lead us to ask ourselves whether nematic configurations with director orientations different from homeotropic can be more stable, which would imply that some of the solutions shown in Fig. 4 are only metastable. In

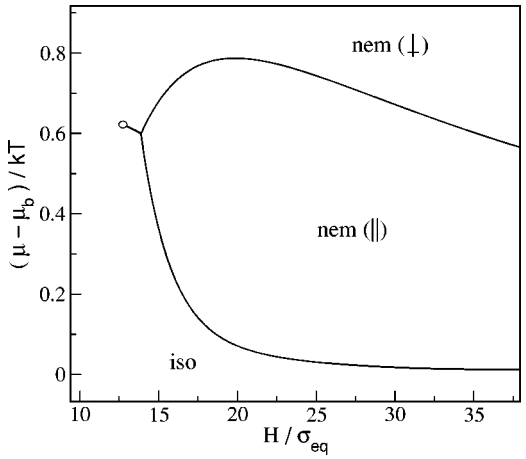

FIG. 8. Surface phase diagram in the chemical potential (μ)–pore width (H) plane for the case $V_0/kT=0.3$. Stability regions where nematic (''nem'') and isotropic (''iso'') states are stable are indicated. In the case of the nematic phases the orientation of the director with respect to the wall ($\perp$ for homeotropic alignment and $\parallel$ for parallel alignment) is also indicated. The open circle indicates the location of a critical point. Substrate decay inverse length was taken to be $\alpha=0.3\sigma_{\mathrm{eq}}^{-1}$.

order to check whether this is the case, we have performed minimizations where the nematic director is constrained to a parallel configuration. The case $V_0/kT=0.13$ with homeotropic alignment (the one shown in Fig. 4) is in fact stable, whereas the case $V_0/kT=0.20$ is not (i.e., the more stable configuration is that with parallel orientation, in complete accord with the behavior dictated by the anchoring transition in the semi-inifinite system); this is represented in Fig. 4 by the dashed line indicating the location of the capillary transition.

How is the phase behavior modified when a true minimization, searching for the global minimum, is performed? Figure 8 shows the surface phase diagram for the case $V_0/kT=0.3$, a much clearer case than $V_0/kT=0.2$ since it is right in the middle of the window between the semi-infinite anchoring transition and the wetting transition. Interestingly, the two structures can be stabilized, and a new phase transition appears. There is an island of nematic states with the director parallel to the walls, separated via first-order phase transitions from isotropic states at lower chemical potentials and nematic states with homeotropic alignment at higher chemical potentials. A third transition line separates isotropic and nematic states with homeotropic orientation, a line which terminates in a critical point, and the three phases coexist at a triple point (H_t,μ_t). The phase transition between the two nematic phases can be considered to be a remnant of the anchoring transition that exists in the semi-infinite fluid out of coexistence with the isotropic phase. Note that this anchoring transition line nem ($\parallel$)–nem ($\perp$) is expected to tend to a value $\mu_A>\mu_b$ for $H\to\infty$. By contrast, the iso–nem ($\parallel$) transition line follows an asymptotic law based on the Kelvin equation and tends to μ_b at $H\to\infty$.

The values of V_0 for which the phase diagram has been plotted in Fig. 4 are about the value $V_0^{\mathrm{WN}\perp}=0$ corresponding to one of the wetting transitions in the semi-infinite system; this transition involves the growth of a wetting layer with the director perpendicular to the substrate and is (or is close to be) of second order. Therefore, no prewetting transition occurs in the semi-infinite system, and no prewetting transition is expected to occur when the system is confined. This situation will be seen to change when considering the case where the substrate favours a parallel orientation for the nematic director: here the transition is first order and a prewetting transition takes place in the semi-infinite system. An interesting question is how this prewetting transition survives for the confined system.

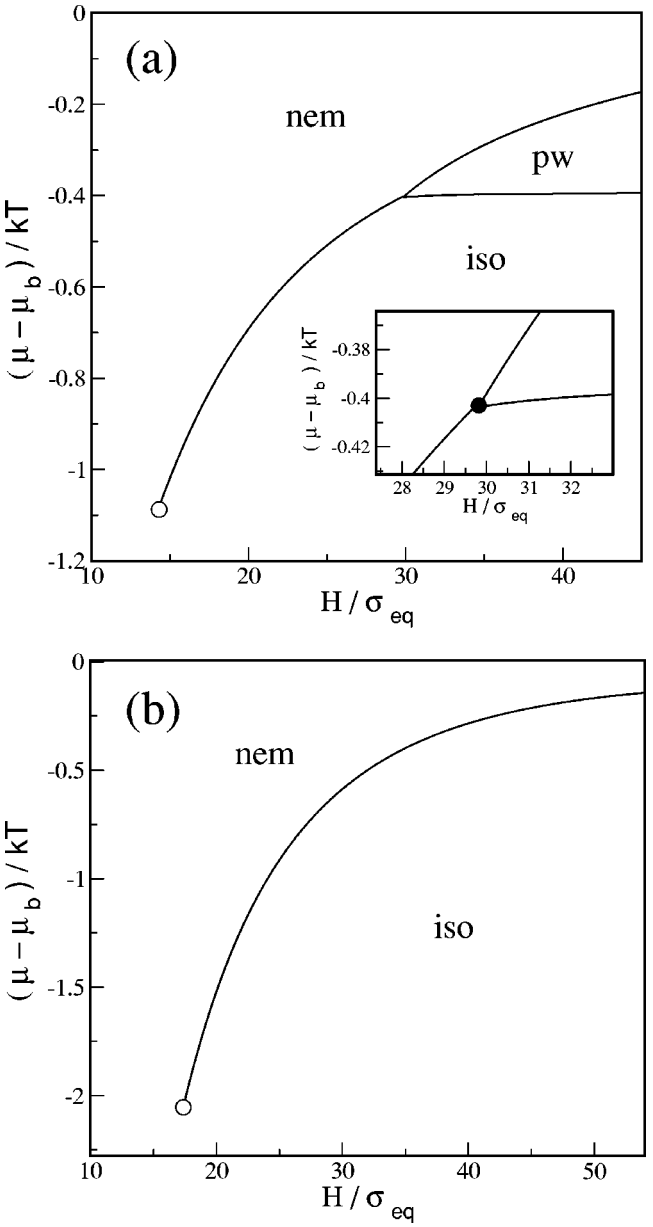

FIG. 9. Surface phase diagram in the chemical potential (μ)–pore width (H) plane for the case of parallel alignment. The chemical potential is referred to the coexistence value μ_b and expressed in thermal energy units. Lines indicate the location of different phase transitions. (a) $V_0/kT=0.7$; nematic (''nem''), isotropic (''iso'') and prewetting (''pw'') states are indicated, and the inset shows an enlargement of the region around the triple point, marked by a black dot. (b) $V_0/kT=1.4$; labels as in the previous case. Substrate decay inverse length was taken to be $\alpha=0.3\sigma_{\mathrm{eq}}^{-1}$.

The surface phase diagram for this case is depicted in Fig. 9 in the chemical potential (μ)–pore width (H) plane, using $V_0/kT=0.7$ in Fig. 9(a) and $V_0/kT=1.4$ in Fig. 9(b).

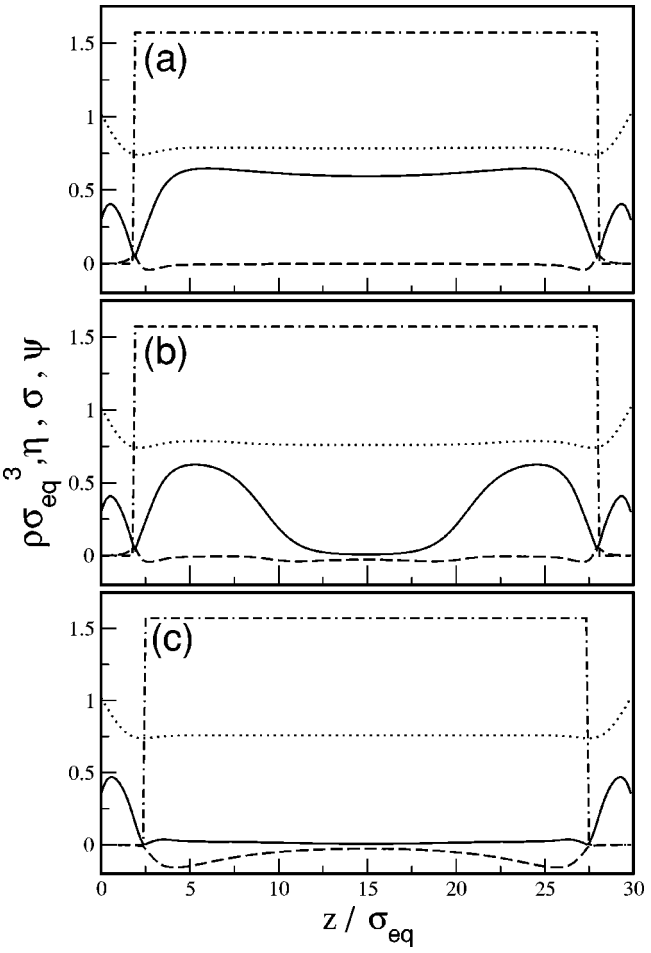

FIG. 10. Density and nematic order-parameter profiles for the case $V_0/kT=0.7$. The three sets of profiles correspond to the three phases that coexist at the triple point shown in Fig. 9(a), i.e., (a) nematic phase ["nem" in Fig. 9(a)]; (b) thin-film phase ("pw"); and (c) isotropic phase ("iso"). Continuous lines: uniaxial order parameter η; dotted lines: number density ρ; dashed lines: biaxial order parameter σ; and dot-dashed lines: tilt angle ψ. Value of the substrate decay inverse length α as in Fig. 4.

Lines indicate the location of first-order phase transitions separating the isotropic ("iso"), nematic ("nem") and isotropic phase with a prewetting layer ("pw") in the case $V_0/kT=0.7$. In this case the prewetting line crosses the capillary nematization line at a triple point where the above three phases coexist. This line has a very small positive slope with H, meaning that the prewetting transition is slightly affected by confinement when the pore is very narrow. In the limit $H\to\infty$ the prewetting line asymptotically tends to the prewetting transition of the semi-infinite system, with only one substrate. The prewetting transition ends at the triple point; beyond this point, i.e., for narrower pores, there is not enough room for the two thick films, one at each substrate, to develop, and the system directly passes to the nematic phase. The capillary isotropic–nematic phase transition continues down to a critical point, below which there is no distinction between both phases. For the case $V_0/kT=1.4$ no prewetting transition line was detected since V_0 is larger than the value for which the prewetting line terminates at the prewetting surface critical point (estimated to be $V_0^{PW}\approx 0.85$). This behavior is similar to that already predicted by Sheng[3] in 1982, using a Landau–de Gennes–type theory suitable for thermotropic liquid crystals.

Figure 10 shows the density and nematic order-parameter profiles for the case $V_0/kT=0.7$ at the triple point shown in Fig. 9(a). The three sets of profiles correspond to the three phases that coexist at the triple point: a nematic phase ("nem"), where the pore is filled with nematic; a phase with thin nematic films close to the two walls ("pw"); and an isotropic phase ("iso"). The two structures that coexist along the prewetting line that develops from the triple point for increasing pore widths are very similar to those coexisting at the corresponding semi-infinite prewetting transition.

The cases presented correspond to situations well inside the region of complete wetting by a nematic phase with parallel director alignment (the wetting transition is estimated to be at $V_0^{WN\parallel}/kT=0.48$). According to the argument based on the Kelvin equation, we expect a standard capillary nematization transition here, with the transition occurring for values of the chemical potential lower than the coexistence value. In the régime of partial wetting, but close to this wetting transition, we should expect the same type of behavior as explained in the previous section, with a region of capillary isotropisation. Figure 11 depicts schematically the type of surface phase diagrams of the confined system studied as a function of V_0.

IV. SUMMARY

In this paper we have investigated the confinement properties of a fluid of hard spherocylinders between two identical parallel substrates using a version of density-functional theory. The substrates act as hard walls on the centers of mass of the particles, while a superimposed orienting field is added which controls the preferred alignment of the nematic

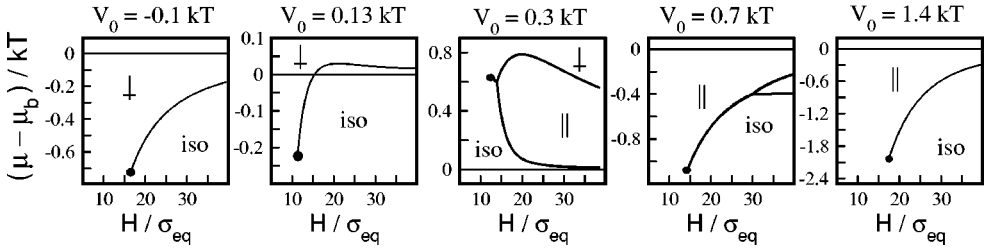

FIG. 11. Summary of the different phase diagrams of the confined fluid in the $\mu-H$ plane as a function of V_0. "iso:" isotropic phase. "⊥:" nematic phase with homeotropic director alignment. "∥:" nematic phase with parallel director alignment.

director. Confinement shifts the chemical potential for the nematic–isotropic transition in a quantity $\Delta\mu$ with respect to the bulk value. In complete agreement with a macroscopic Kelvin-type analysis, the shift may be toward lower chemical potential, $\Delta\mu<0$—standard capillary transition—or toward higher chemical potential, $\Delta\mu>0$, giving rise to a *reversed* capillary transition or capillary isotropization transition. The occurrence of one type of transition or the other is dictated by which is phase, either isotropic or nematic, that the substrate prefers or, in other words, by the sign of the cosine of the contact angle, $\cos\theta_c$. Since this system presents two wetting transitions by nematic phases, $\cos\theta_c$ may change sign twice, and consequently two changes of regime, from a standard to a reversed capillary transition and then back to a standard transition, take place. Ultimately, then, this behavior is associated with the wetting properties of the semi-infinite system, which do not appear explicitely in the confined system (since the system does not have enough space to develop infinitely-thick nematic layers) but only indirectly. Another effect of the bulk wetting transition is the persistence of the prewetting transition in the confined system. Finally, the anchoring transition that occurs in the semi-infinite system and that spans a certain range in chemical potential in the nematic region of stability, survives in the confined system, and modifies the behavior of the confined fluid in an interesting manner. The present results have the value of somehow unifying different behaviors of the semi-infinite system when the system is confined by parallel walls, using a completely microscopic approach.

Future work involves the implementation of the full Somoza–Tarazona[18] density-functional theory which includes an averaged density profile and is therefore capable of describing highly structured density profiles. This model is therefore expected to give a more faithful representation of the system when the pore width is very much reduced and the liquid-mediated interaction between the walls is important. Also, the model can account for the strongly inhomogeneous structures typical of smectic phases. These calculations may prove very interesting since it is expected that conmensuration effects associated with the layer spacing of the smectic phase and the pore width will play a crucial role in establishing the equilibrium structure of the system and may induce an extremely rich surface phase diagram.

ACKNOWLEDGMENTS

We thank Professor Navascués for illuminating discussions. This work was partially supported by Grants No. BFM2001-0224-C02-01, No. BFM2001-0224-C02-02, and No. BFM2001-1679-C03-02 (Spain). D. de las H. is supported by a FPU grant from The Spanish Ministry of Education and Culture.

[1] B. Jérôme, Rep. Prog. Phys. **54**, 391 (1991).
[2] T. J. Sluckin and A. Poniewierski, in *Fluid Interfacial Phenomena*, edited by C. A. Croxton (Wiley, Chichester, 1986), Chap. 5, and references therein.
[3] P. Sheng, Phys. Rev. Lett. **37**, 1059 (1976); Phys. Rev. A **26**, 1610 (1982).
[4] A. Poniewierski and T. J. Sluckin, Liq. Cryst. **2**, 281 (1987).
[5] K. E. Gubbins, Rep. Prog. Phys. **62**, 1573 (1999).
[6] K. Kocevar, A. Borstnik, I. Musevic, and S. Zumer, Phys. Rev. Lett. **86**, 5914 (2001).
[7] D. de las Heras, L. Mederos, and E. Velasco, Phys. Rev. E **68**, 031709 (2003).
[8] G. D. Wall and D. J. Cleaver, Phys. Rev. E **56**, 4306 (1997).
[9] M. P. Allen, J. Chem. Phys. **112**, 5447 (2000).
[10] I. Rodríguez-Ponce, J. M. Romero-Enrique, E. Velasco, L. Mederos, and Luis F. Rull, J. Phys.: Condens. Matter **12**, A363 (2000).
[11] P. I. C. Teixeira, A. Chrzanowska, G. D. Wall, and D. J. Cleaver, Mol. Phys. **99**, 889 (2001).
[12] I. Rodríguez-Ponce, J. M. Romero-Enrique, and Luis F. Rull, Phys. Rev. E **64**, 051704 (2001)
[13] J. Quintana, E. C. Poire, and H. Dominguez, Mol. Phys. **100**, 2597 (2002).
[14] A. Chrzanowska, P. I. C. Teixeira, H. Ehrentraut, and D. J. Cleaver, J. Phys.: Condens. Matter **13**, 4715 (2001).
[15] R. van Roij, M. Dijkstra, and R. Evans, Europhys. Lett. **49**, 350 (2000).
[16] R. van Roij, M. Dijkstra, and R. Evans, J. Chem. Phys. **113**, 7689 (2000).
[17] M. Dijkstra, R. van Roij, and R. Evans, Phys. Rev. E **63**, 051703 (2001).
[18] A. M. Somoza and P. Tarazona, Phys. Rev. Lett. **61**, 2566 (1988); J. Chem. Phys. **91**, 517 (1989).
[19] E. Velasco, L. Mederos, and D. E. Sullivan, Phys. Rev. E **62**, 3708 (2000).
[20] E. Velasco, L. Mederos, and D. E. Sullivan, Phys. Rev. E **66**, 021708 (2002).
[21] L. Onsager, Ann. N.Y. Acad. Sci. **51**, 627 (1949).